
Numerical study of heat transfer and pressure drop in a fuel cell with porous material

Afshin Shiriny, Morteza Bayareh*

Department of Mechanical Engineering, Shahrekord University, Shahrekord, Iran
m_bayareh@yahoo.com

ABSTRACT. *The purpose of this research is to cool the polymer fuel cells using a cooling fluid. The use of metal porous materials in fluid channels increases the level of fluid contact with the thermal surface. Porous metals are used inside the channels with spiral, parallel and multi-channel arrangement. Heat transfer and pressure drop are investigated for different materials, different porosities, and various arrangements of the full cell. Two fluids, water and ethylene glycol are used as a working fluid. The results show that the water has a better thermal performance. As the porosity of the material increases, the heat transfer and the pressure drop decreases. It is revealed that the multi-channel arrangement has the highest heat transfer rate, while the spiral pattern shows the highest pressure drop.*

RÉSUMÉ. *Le but de cette recherche est de refroidir les piles à combustible à polymère à l'aide d'un fluide de refroidissement. L'utilisation de matériaux métalliques poreux dans les canaux de fluide augmente le niveau de contact du fluide avec la surface thermique. Les métaux poreux sont utilisés à l'intérieur des canaux avec une disposition en spirale, parallèle et multicanal. Le transfert de chaleur et la chute de pression ont été étudiés pour différents matériaux, différentes porosités et divers arrangements du combustible complet. Deux fluides, l'eau et l'éthylène glycol sont utilisés comme fluide de travail. Les résultats montrent que l'eau a une meilleure performance thermique. Au fur et à mesure que la porosité du matériau augmente, le transfert de chaleur et la perte de charge diminuent. Il est révélé que la configuration à canaux multiples présente le taux de transfert de chaleur le plus élevé, tandis que le motif en spirale présente la perte de charge la plus élevée.*

KEYWORDS: *fuel cell, porous material, heat transfer, pressure drop.*

MOTS-CLÉS: *pile à combustible, matériau poreux, transfert de chaleur, chute de pression.*

DOI:10.3166/ACSM.42.323-334 © 2018 Lavoisier

1. Introduction

Polymer electrolyte fuel cells (PEFCs) as a renewable energy source have attracted much interest. The membrane that is a main component of a PEFC should be wet for proper operation and its drying results in a reduction in its performance. Thus, the cooling of this equipment and rejection of the heat is of great importance. One of the most commonly used methods is the use of refrigerants in the channels (Nimvari *et al.*, 2012). The cooling efficiency increases by increasing the contact area between the fluid and the surfaces. In this paper, this is achieved by using porous materials for channels. In the fuel cell, the fuel and oxidant are continuously injected and need no recharging. The full cell consists of a porous cathode, a porous anode and an electrolyte. They generate a considerable amount of heat (Kanda *et al.*, 2013). Therefore, the generated heat should be well rejected to prevent overheating of the components especially the membrane. In other words, the performance of the cell at the optimum membrane temperature is high (Erkinaci and Baytas, 2017). It is worth noting that the optimum temperature range of the membrane is not only related to high temperatures. On the other hand, the operating temperature should not be lower than its optimal value. If this occurs, the phenomenon of flooding occurs, which have an adverse effect on the performance of the fuel cell (Barbir *et al.*, 1999). There are various methods for cooling the fuel cell include natural convection, cooling through the excess air blown into the cathode, cooling by the heat exchangers, phase change of the refrigerant, etc. (Jiao and Li, 2011). Choi *et al.* (2008) optimized the cooling field to improve thermal performance of the fuel cell. Their research showed that heat rejection from different parts was influenced by the distribution of fluid with different arrangements. Yu *et al.* (2009) studied the effects of Reynolds number and heat flux in a spiral-cooled coil flow field numerically. Their results demonstrated that the use of several spiral paths is better than ordinary simple spiral one. Baek *et al.* (2011) numerically simulated of uniform cooling of large-scale PEMFCs with different coolant flow field designs. Their results showed that temperature distribution varies for different designs. Kurnia *et al.* (2011) analyzed various fields include spiral, parallel, wavy, and gear ones in a laminar regime under a constant heat flux. Asghari *et al.* (2011) investigated the parallel-spiral plan, taking into account the number of parallel paths as a design parameter numerically and experimentally. They compared the fluid thermal behavior of different designs and stated that optimizing the coolant field can be performed by different optimal designs. Gould *et al.* (2014) studied the cooling of the fuel cell and compared a numerical model with infrared imaging. They concluded that infrared imaging could be very effective to study the flow field. Islam *et al.* (2016) used water and ethylene glycol as working fluids and found that using nanofluid can be significantly reduced the size of heat exchanger and pump power. Zakaria *et al.* (2016) investigated the cooling of the fuel cell using water- Al_2O_3 and ethylene glycol- Al_2O_3 nanofluids. They used a parallel flow field at different Reynolds numbers under constant heat flux. Singdeo *et al.* (2017) improved the spiral cooling field using a three-dimensional simulations. Rahgoshay *et al.* (2017) studied the cooling of the fuel cell for two parallel and spiral arrangements. They analyzed parameters such as pressure drop, heat rejection, and maximum temperature, and indicated that the spiral plan exhibits higher performance at different operating

temperatures. Choi *et al.* (2017) studied cooling and humidification in a fuel cell by injection water experimentally. They found that the polarity and dew point of gas are important parameters. It was revealed that increasing the temperature of the water and the humidity increase the performance of the fuel cell.

The main objective of the present study is to use porous materials inside the channels for spiral, parallel and multi-channel arrangements of the fuel cell. Heat transfer and pressure drop are investigated for different variables such as the porosity and type of the fluid. A three-dimensional model of the serpentine channel, which consists of a porous region inside the channel, a graphite plate below the heat flux, input and output regions (Figure 1). The channel inlet area is $1\text{ mm} \times 1\text{ mm}$.

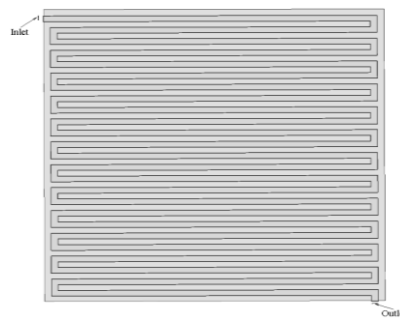


Figure 1. Physical model of the serpentine channel

Water or ethylene glycol are selected as a fluid that enter the inlet area and then pass through the channel with porous material exit from the outlet section. The heat transfers to the fluid through a graphite layer. Figure 2 shows the location of the cooling channels, which are filled with porous materials.

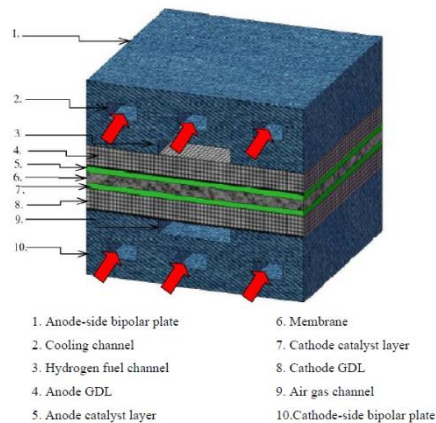


Figure 2. Schematic of the fuel cell

The remainder of this paper is organized as follows: in section 2, the governing equations are described. The results are presented in section 3 and the concluding remarks are introduced in section 4.

2. Governing equations

The porous medium is an inhomogeneous system composed of a solid matrix and empty spaces along with fluid motion and can be considered as a continuous environment. The fluid is assumed to be incompressible and the thermal equilibrium is established between the fluid and solid phases. The governing equations are continuity, the Navier-Stokes and the energy are defined as follows, respectively (Nimvari *et al.*, 2012):

$$\nabla \cdot \vec{u} = 0 \quad (1)$$

$$(2)$$

$$\sigma \frac{\partial T}{\partial t} + \vec{u} \cdot \vec{\nabla} T = \vec{\nabla} \cdot (\alpha_m \vec{\nabla} T) \quad (3)$$

where $\vec{u} = (\bar{u}, \bar{v})$, p and T are the velocity vector, the pressure, and the temperature, respectively. ν_e is the effective viscosity, ε the porosity coefficient and α_m effective thermal expansion coefficient in porous material that is defined as follows:

$$\alpha_m = \frac{(1 - \varepsilon)k_s + \varepsilon k_f}{(\rho c_p)_f} \quad (4)$$

where k_f and k_s are the conductivity of the fluid and solid phases, respectively. In addition, σ is the coefficient of thermal capacity of solid and fluid and is defined as:

$$\sigma = \varepsilon + \frac{(1 - \varepsilon)\rho_s c_{ps}}{\rho_f c_{pf}} \quad (5)$$

where ρ_f and ρ_s are the fluid and solid density, respectively. c_{pf} and c_{ps} are the heat capacity at constant pressure for fluid and solid phases, respectively. The force vector \vec{F} is due to the presence of porous material and other external forces calculated as follows:

$$\vec{F} = -\frac{\varepsilon \nu}{k} \vec{u} - \frac{\varepsilon F_\varepsilon}{\sqrt{K}} |\vec{u}| \vec{u} + \varepsilon \vec{G} \quad (6)$$

where F_ε is the geometric function and K is the permeability of the porous material that are defined as follows, respectively:

$$F_\varepsilon = \frac{1.75}{\sqrt{150\varepsilon^3}} \quad (7)$$

$$K = \frac{\varepsilon^3 D_p^2}{150(1-\varepsilon)^2} \quad (8)$$

ν is the viscosity of the fluid and \vec{G} is calculated from the following equation:

$$\vec{G} = -\vec{g}\beta(T - T_0) + \vec{a} \quad (9)$$

where \vec{g} is the gravitational acceleration and β is the volumetric expansion coefficient.

Since the line $r = 0$ is the axis of symmetry of tube, the radial and the axial velocity components are zero. The no-slip boundary condition is used on the pipe wall; this means that all variables except the temperature on the wall of are considered zero. The boundary conditions at the inlet and outlet are velocity inlet and pressure outlet, respectively. The input fluid temperature is 283 K. the fluid flow is considered as creeping one. The graphite plates are considered as wall boundary conditions with a constant heat flux of 1000 W/m^2 . The porosity percentages of 60, 70, 80 and 90 are investigated. Also, the size of the porosity region is assumed to be 1 mm.

3. Results

3.1. Grid independency

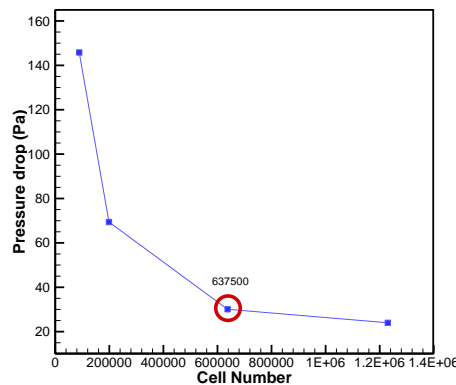


Figure 3. Pressure drop between inlet and outlet of the fuel cell for different grid resolutions

In this section, the resolution of the computational grid is evaluated. The appropriate number of grid points has a great impact on the accuracy of the numerical simulations. In order to test the effect of the number of grid points on numerical results, various grid resolutions are considered. The results are shown in Figure 3 in which the pressure drop is compared between the input and output of the fuel cell. The results show that the number of 637,500 grid points is enough for the present simulation.

3.2. Validation

In this study, a simulation is performed for validation and the results are compared with the ones of Baek *et al.* (2011) who studied heat transfer in a serpentine multi-channel of $2 \times 2 \times 1 \text{ mm}^3$ with a graphite plate of $180 \times 180 \times 2 \text{ mm}^3$. The volume flow rates of 2×10^{-6} , 4×10^{-6} and $6 \times 10^{-6} \text{ lit/min}$ are considered in accordance with the reference work. It should be noted that the parameters studied in validation are similar to those of the model B of the reference article Baek *et al.* (2011). The results show that the present simulations are in good agreement with the results of Baek *et al.* (2011).

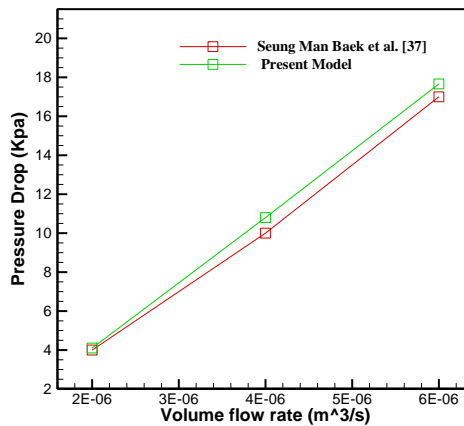


Figure 4. Pressure drop as a function of volume flow rate

3.3. Effect of the porosity of the serpentine channel on the Nusselt number

In this section, water is used as the working fluid and aluminum is used as the porous medium. The porosity value is 0.9 and the diameter of the porosity cavity is equal to 0.0025 m. As shown in Figure 5, the Nusselt number increases with increasing the inlet volume flow rate. This increase is due to an increase in the natural convection (an increase in fluid momentum). By adding a porous medium to the fluid channel, the contact area between the fluid and the porous medium increases results in an increase in the heat transfer. The increase in the Nusselt number is higher for larger volume flow rate.

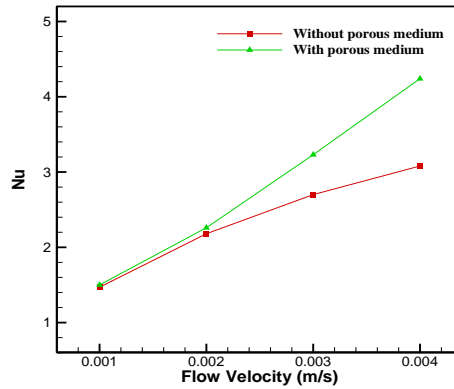


Figure 5. The Effect of porosity of the serpentine channel on the Nusselt number

The effect of porosity of 0.6, 0.7, 0.8 and 0.9 on the Nusselt number is plotted in Figure 6. The diameter of the porous cavity is equal to 0.0025 m, the heat flux is 1000 W/m^2 , and the water is considered at 283 K. According to the results, the amount of heat transfer decreases with the porosity. The cross-sectional flow of fluid through the cavities increases by increasing the porosity with the same fluid flow rate. Therefore, the momentum of the fluid decreases in those areas. This reduction in momentum leads to a reduction in the heat transfer.

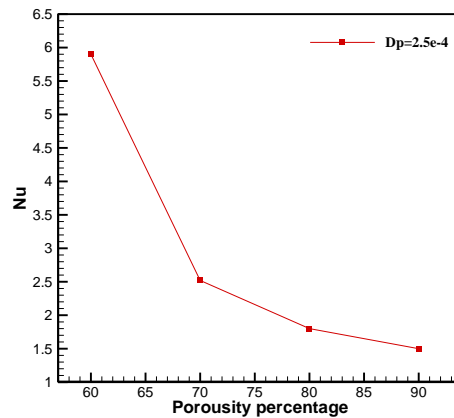


Figure 6. The effect of porosity percentage on the Nusselt number

The temperature contours are presented in Figure 7 for different porosity percentages. The porosity ratios are considered to be 0.6, 0.7, 0.8 and 0.9 and the water temperature is 283 K. As the temperature contours show, the heat transfer rate decreases with increasing the porosity.

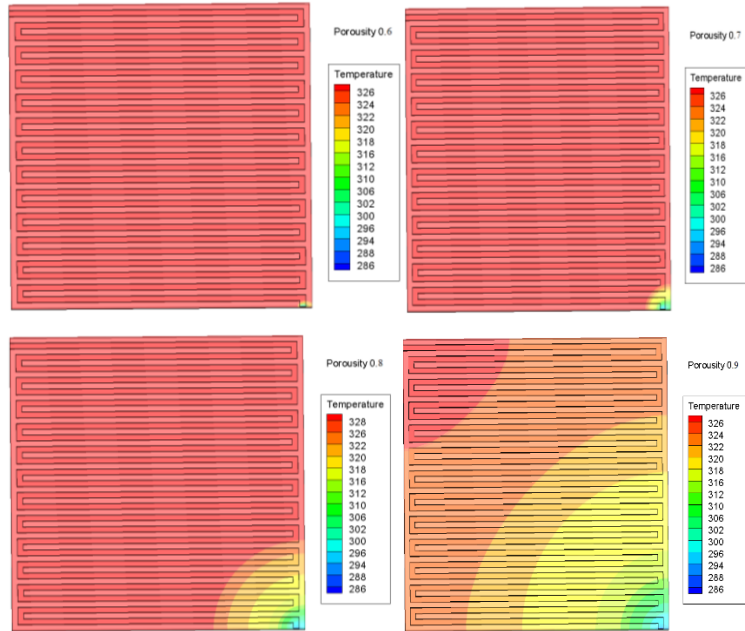


Figure 7. Temperature contours across the fuel cell for different porosity percentages

3.4. Effect of the working fluid on the Nusselt number

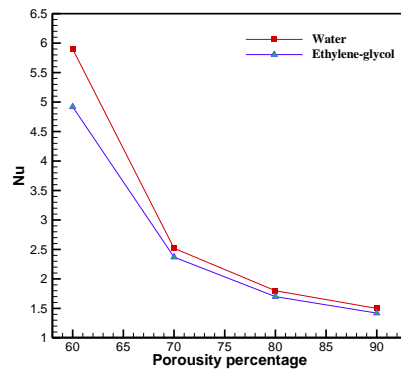


Figure 8. Effect of working fluid on the Nusselt number

In this section, the effects of ethylene glycol and water as the two most commonly used working fluids are investigated. The porosity values are 0.6, 0.7, 0.8 and 0.9 and

the inlet temperature is 283 K. The diameter of the porosity cavity is equal to 0.3025 meters. The results are shown in Figure 8. According to the results, the heat transfer for ethylene glycol as a working fluid is less than that for water. The reason for this is the higher amount of heat transfer coefficient of water (0.6 W/mK) compared to the ethylene glycol heat transfer coefficient (0.262 W/mK).

3.5. Effect of channel design on the Nusselt number

A schematic of three types of serpentine, parallel, and multi-channel arrangements is shown in Figure 9. In this section, the water fluid at 283 K is entered into each of the channels, and the porosity ratio is 0.9, 0.8, 0.7 and 0.6 and the diameter of the porosity cavity is equal to 0.225 m. The results are shown in Figure 10. According to the results, the amount of heat transfer in the arrangement of the multi-channel spiral plan is more than the rest of the channels. In fact, in this scheme, the fluid has enough time for exchange the heat in comparison with the other arrangements.

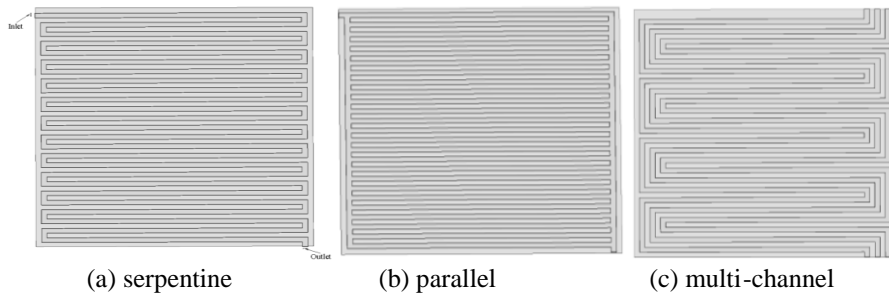


Figure 9. Schematic of different cooling channels

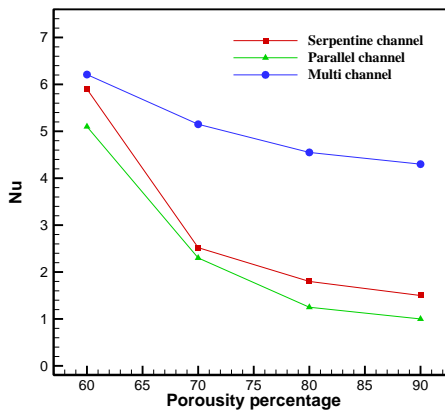


Figure 10. The effect of the channel type containing porous material on the Nusselt number

3.6. Effect of channel design on pressure drop

In this section, three types of serpentine, parallel and multi-channel arrangements are used to calculate the pressure drop. The porosity percentages of 0.6, 0.7, 0.8 and 0.9 are considered. The water inlet temperature is 283 K. The results are shown in Figure 11. The pressure drop in the serpentine channel is higher than that in other channels. This is due to the higher length of the fluid path through the spiral channel.

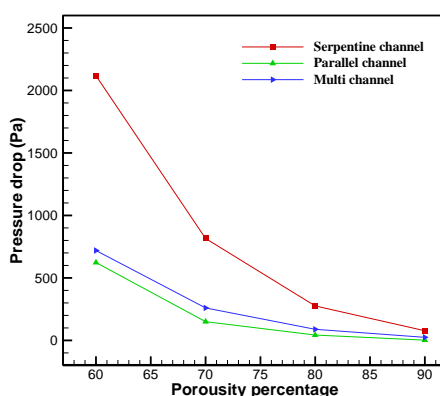


Figure 11. Effect of channel design containing porous medium on the pressure drop

4. Conclusions

In this research, the effect of the porosity on the heat transfer and pressure drop in a fuel cell was investigated. The results revealed that increasing the volume flow rate leads to an increase in the Nusselt number. Also, the channel containing the porous material shows higher pressure drop than the simple channel without the porosity. The heat transfer and the pressure drop decrease with increasing the porosity. The use of water as a channel inlet fluid has a higher heat transfer than ethylene glycol one. Also, the pressure parameter for the case of water is lower than that for ethylene glycol. The results demonstrated that the highest heat transfer corresponds to the Multi-channel design and the highest pressure drop is related to serpentine one.

References

- Asghari S., Akhgar H. (2011). Design of thermal management subsystem for a 5KW polymer electrolyte membrane fuel cell system. *Journal of Power Sources*, Vol. 196, No. 6, pp. 3141-3148. <http://dx.doi.org/10.1016/j.jpowsour.2010.11.077>
- Baek S. M., Yu S. H., Nam J. H., Kim C. J. (2011). A numerical study on uniform cooling of large-scale PEMFCs with different coolant flow field designs. *Applied Thermal Engineering*, Vol. 31, pp. 1427-1434. <http://dx.doi.org/10.1016/j.applthermaleng.2011.01.009>

- Barbir F., Braun J., Neutzler J. (1999). Properties of molded graphite bi-polar plates for PEM fuel cells. *International Journal on New Materials for Electrochemical Systems*, Vol. 2, pp. 197-200.
- Choi E. J., Hwang S. H., Park J., Kim M. S. (2017). Parametric analysis of simultaneous humidification and cooling for PEMFCs using direct water injection method. *International Journal of Hydrogen Energy*, Vol. 42, No. 17, pp. 12531-12542. <http://dx.doi.org/10.1016/j.ijhydene.2017.03.201>
- Choi J., Kim Y. H., Lee Y., Lee K. J., Kim Y. (2008). Numerical analysis on the performance of cooling plates in a PEFC. *Journal of Mechanical Science and Technology*, Vol. 22, No. 7, pp. 1417-1425. <http://dx.doi.org/10.1007/s12206-008-0409-6>
- Erkinaci T., Baytas F. (2017). CFD investigation of a sensible packed bed thermal energy storage with different porous materials. *International Journal of Heat and Technology*, Vol. 35, pp. S281-S287. <http://dx.doi.org/10.18280/ijht.35Sp0128>
- Gould B. D., Ramamurti R., Osland C. R., Swider-Lyons K. E. (2014). Assessing fuel-cell coolant flow fields with numerical models and infrared thermography. *International Journal of Hydrogen Energy*, Vol. 39, pp. 14061-14069. <http://dx.doi.org/10.1016/j.ijhydene.2014.07.018>
- Islam M. R., Shabani B., Rosengarten G. (2016). Nanofluids to improve the performance of PEM fuel cell cooling systems: A theoretical approach. *Applied Energy*, Vol. 178, pp. 660-671. <http://dx.doi.org/10.1016/j.apenergy.2016.06.090>
- Jiao K., Li X. (2011). Water transport in polymer electrolyte membrane fuel cells. *Progress in Energy and Combustion Science*, Vol. 37, No. 3, pp. 221-291. <http://dx.doi.org/10.1016/j.pecs.2010.06.002>
- Kanda D., Watanabe H., Okazaki K. (2013). Effect of local stress concentration near the rib edge on water and electron transport phenomena in polymer electrolyte fuel cell. *International Journal of Heat and Mass Transfer*, Vol. 67, pp. 659-665. <http://dx.doi.org/10.1016/j.ijheatmasstransfer.2013.08.065>
- Kurnia J., Sasmito A. P., Mujumdar A. S. (2011). Numerical investigation of laminar heat transfer performance of various cooling channel designs. *Applied Thermal Engineering*, Vol. 31, pp. 1293-1304. <http://dx.doi.org/10.1016/j.applthermaleng.2010.12.036>
- Nimvari M. E., Maerefat M., El-Hossaini M. K. (2012). Numerical simulation of turbulent flow and heat transfer in a channel partially filled with a porous media. *International Journal of Thermal Sciences*, Vol. 60, pp. 131-141. <http://dx.doi.org/10.1016/j.ijthermalsci.2012.05.016>
- Rahgoshay S. M., Ranjbar A. A., Ramiar A., Alizadeh E. (2017). Thermal Investigation of a PEM fuel cell with cooling flow field. *Energy*, Vol. 134, pp. 61-73. <http://dx.doi.org/10.1016/j.energy.2017.05.151>
- Singdeo D., Dey T., Gaikwad S., Andreasen S. J., Ghosh P. C. (2017). A new modified-serpentine flow field for application in high temperature polymer electrolyte fuel cell. *Applied Energy*, Vol. 195, pp. 13-22. <http://dx.doi.org/10.1016/j.apenergy.2017.03.022>
- Yu S. H., Sohn S., Nam J. H., Kim C. J. (2009). Numerical study to examine the performance of multi-pass serpentine flow fields for cooling plates in polymer electrolyte membrane fuel cells. *Journal of Power Sources*, Vol. 194, pp. 697-703. <http://dx.doi.org/10.1016/j.jpowsour.2009.06.025>

Zakaria I., Azmi W. H., Mamat A. M. I., Mamat R., Saidur R., Abu Talib S. F., Mohamed W. A. N. W. (2016). Thermal analysis of Al₂O₃ water ethylene glycol mixture nanofluid for single PEM fuel cell cooling plate: An experimental study. *International Journal of Hydrogen Energy*, Vol. 41, pp. 5096-5112.
<http://dx.doi.org/10.1016/j.ijhydene.2016.01.041>